Search for scalar-tensor mixed polarization modes of gravitational waves

Hiroki Takeda,[1,2,*] Soichiro Morisaki,[3] and Atsushi Nishizawa[4]

[1]*Department of Physics, Kyoto University, Kyoto 606-8502, Japan*
[2]*Department of Physics, University of Tokyo, Bunkyo, Tokyo 113-0033, Japan*
[3]*Department of Physics, University of Wisconsin-Milwaukee, Milwaukee, Wisconsin 53201, USA*
[4]*Research Center for the Early Universe (RESCEU), School of Science, University of Tokyo, Bunkyo, Tokyo 113-0033, Japan*

(Received 7 May 2021; accepted 24 March 2022; published 12 April 2022)

An additional scalar degree of freedom for a gravitational wave is often predicted in theories of gravity beyond general relativity and can be used for a model-agnostic test of gravity. In this article, we report the direct search for the scalar-tensor mixed polarization modes of gravitational waves from compact binaries in a strong regime of gravity by analyzing the data of GW170814 and GW170817, which are the merger events of binary black holes and binary neutron stars, respectively. Consequently, we obtain the constraints on the ratio of scalar-mode amplitude to tensor-mode amplitude: $\lesssim 0.10$ for GW170814 and $\lesssim 0.034$ for GW170817, which are the tightest constraints on the scalar amplitude in a strong regime of gravity before merger.

DOI: 10.1103/PhysRevD.105.084019

I. INTRODUCTION

General relativity (GR) has passed all experimental and observational tests so far [1–3]. However, many alternative theories of gravity have been suggested and studied for various theoretical motivations [4,5]. For example, a scalar-tensor theory [6,7] is one of the simplest extensions of GR and some models are motivated from the late-time accelerating expansion of the Universe [8]. It is well known that a gravitational wave (GW) can have two tensor degrees of freedom in GR, while the scalar-tensor theory additionally introduces scalar degrees of freedom for a GW via scalar fields [1,9]. The scalar polarization modes of a GW are also predicted in $f(R)$ gravity [10]. It has been pointed out that scalar-tensor polarization mixing can occur in the gravitational lensing beyond GR [11]. In this way, the degrees of freedom of a GW reflect the nature of gravity. Any signature of nontensorial polarization modes that are forbidden in GR demands the extensions of GR if they are discovered [12].

The observations of GWs from compact binary coalescences [13,14] by advanced LIGO [15] and advanced Virgo [16] have been able to test GR in a stronger gravity regime [17–19]. Some analytical and numerical studies to probe into the anomalous polarization modes have been made for GWs from compact binary coalescences [20–26]. So far, the polarization modes of GWs from compact binary coalescences have been tested in the pure polarization framework, in which one performs the model selection between GR and an extreme case of an alternative gravity theory allowing only scalar or vector polarization modes. In the context of such pure polarization tests, the signals of GW170814 [19] and GW170817 [27] strongly favor the tensor polarization against the pure vector or scalar polarizations [19,28,29]. On the other hand, the polarization test based on the null stream method that does not require any waveform of a GW has been performed [18,23,24]. The result supports GR modestly.

However, most of alternative theories of gravity predict tensor modes along with subdominant vector and/or scalar modes. In other words, a detector signal would be typically a mixture of those polarization modes. The most stringent constraint on the additional scalar amplitude has been obtained from the measurement of the orbital period of the binary pulsars and is consistent with the tensor modes in GR [4]. However, it is still in a weak gravity regime much before the merger of the binary. In this article, we probe the amplitude of the extra scalar mode mixed with the ordinary tensor modes for GW170814 and GW170817 in a strong regime of gravity just before the merger. The two binary merger events were detected by three detectors so that we can separate a mixture of the scalar-tensor polarizations, in principle [21]. Our model for the scalar waveform includes both $\ell = 1$ and $\ell = 2$ harmonics, applied only to the inspiral phase of the GW signals from these two events. This is the first analysis that allows an arbitrary mixture of tensor and (model-specific) scalar contributions in the signal hypothesis and is based on a scalar-tensor waveform. Throughout this article we use the geometrical units, $c = G = 1$, and all uncertainties are defined by 90% credible intervals unless they are mentioned explicitly.

*takeda@tap.scphys.kyoto-u.ac.jp

II. SCALAR-TENSOR POLARIZATION MODEL

Some theories of gravity such as the scalar-tensor theory predict the existence of the scalar polarization in addition to the standard tensor modes. The scalar modes can be radiated through dipole and quadrupole patterns. As a waveform-agnostic approach, the reconstruction method, which is capable of detecting and characterizing the mixed polarizations of a transient GW signal, has been proposed in [26,30]. In contrast, our analysis here is based on a parametrized waveform model constructed according to the features commonly seen in the scalar-tensor waveforms in some of typical gravity theories. The approach is not completely model independent but enables us to achieve higher sensitivity to a possible deviation from GR. The waveform has the following features.

(i) The model consists of the scalar and tensor modes. Since the two scalar polarizations (longitudinal and breathing) are completely degenerate for an interferometric detector [21,31], we consider three polarization modes, that is, plus, cross, and one scalar polarization mode.

(ii) The scalar mode has two leading harmonics: dipole and quadrupole. The angular pattern of GW emission, or the inclination-angle ι dependence of the scalar mode, should be proportional to $\sin\iota$ for the dipole radiation and $\sin^2\iota$ for the quadrupole radiation [20,21,29]. From a general consideration of harmonics [20], the ℓth harmonic in the time domain has the parameter dependence,

$$h^{(\ell)}(t) = \eta^{(2-\ell)/5}\frac{\mathcal{M}}{d_L}(2\pi\mathcal{M}F)^{\ell/3}e^{-i\ell\Phi}. \quad (1)$$

We assume that the waveform of the ℓth scalar polarization mode has the ℓth harmonics characterized by the amplitude parameter $A_{S\ell}$. Here, $\mathcal{M}$ is the chirp mass, d_L is the luminosity distance, and η is the symmetric mass ratio. In addition, F and Φ are the orbital frequency and phase, respectively.

(iii) The tensor amplitude and phasing are deformed due to a backreaction from the extra energy loss due to scalar radiation. Let δA and $\delta\Psi$ be the amplitude and phase corrections from the additional energy loss. The resulting modification of the change rate of the binary binding energy can be calculated as

$$\begin{aligned}\dot{E} &= \frac{d_L^2}{32\pi}\int d\Omega\langle \dot{h}_{ij}\dot{h}^{ij}\rangle \\ &= \dot{E}^{\rm GR} + \frac{32}{15}A_{S2}^2 d_L^2\langle\dot{h}^{(2)2}\rangle + \frac{2}{3}A_{S1}^2 d_L^2\langle\dot{h}^{(1)2}\rangle \\ &= \dot{E}^{\rm GR}\left(1+\frac{2}{3}A_{S2}^2 + \frac{5}{96}A_{S1}^2\eta^{2/5}(2\pi\mathcal{M}F)^{-2/3}\right),\end{aligned} \quad (2)$$

where the stress-energy tensor in GR is assumed, $\langle\cdot\rangle$ denotes an averaging procedure, and $\dot{E}^{(\rm GR)}$ denotes the change rate in GR. Keeping up to the second order in terms of A_S, the modification leads to the amplitude and phase corrections as

$$\begin{aligned}\delta A^{(\ell)} &= \delta A_q^{(\ell)} + \delta A_d^{(\ell)} \\ &= -\frac{1}{3}A_{S2}^2 - \frac{5}{192}A_{S1}^2\eta^{2/5}u_\ell^{-2},\end{aligned} \quad (3)$$

$$\begin{aligned}\delta\Psi^{(\ell)} &= \delta\Psi_q^{(\ell)} + \delta\Psi_d^{(\ell)} \\ &= \frac{\ell}{128}A_{S2}^2 u_\ell^{-5} + \frac{5\ell}{14336}A_{S1}^2\eta^{2/5}u_\ell^{-7},\end{aligned} \quad (4)$$

through the stationary phase approximation [20]. The reduced ℓth harmonic frequency is defined as $u_\ell := (2\pi\mathcal{M}f/\ell)^{1/3}$, where $f = \ell F$ is the GW frequency.

(iv) The modification of the conservative dynamics is not introduced. That is because the modifications appear at the same order as the modification by the energy loss and completely degenerate with the amplitude parameters.

Consequently, we obtain the following signal model in the frequency domain and we analyze the data under the scalar-tensor hypothesis $\mathcal{H}_{\rm ST}$,

$$\tilde{h}_I(f,\hat{\Omega}) = \tilde{h}_T^{(2)} + \tilde{h}_S^{(2)} + \tilde{h}_S^{(1)}, \quad (5)$$

$$\begin{aligned}\tilde{h}_T^{(2)} &= -[F_I^+(1+\cos^2\iota) + 2iF_I^\times\cos\iota] \\ &\quad\times(1+\delta A^{(2)})\sqrt{\frac{5\pi}{96}}\frac{\mathcal{M}^2}{d_L}u_2^{-7/2}e^{-i\Psi_{\rm GR}^{(2)}}e^{-i\delta\Psi^{(2)}}\end{aligned} \quad (6)$$

$$\tilde{h}_S^{(2)} = \sqrt{\frac{5\pi}{96}}A_{S2}F_I^b\sin^2\iota\frac{\mathcal{M}^2}{d_L}u_2^{-7/2}e^{-i\Psi_{\rm GR}^{(2)}}e^{-i\delta\Psi^{(2)}} \quad (7)$$

$$\tilde{h}_S^{(1)} = \sqrt{\frac{5\pi}{48}}A_{S1}F_I^b\sin\iota\eta^{1/5}\frac{\mathcal{M}^2}{d_L}u_1^{-9/2}e^{-i\Psi_{\rm GR}^{(1)}}e^{-i\delta\Psi^{(1)}}, \quad (8)$$

where $\tilde{h}_T^{(2)}$, $\tilde{h}_S^{(2)}$, and $\tilde{h}_S^{(1)}$ represent the quadrupole tensor, quadrupole sclalar, and dipole scalar polarization, respectively. $\tilde{h}_S^{(2)}$ and $\tilde{h}_S^{(1)}$ are characterized by their amplitude A_{S2} and A_{S1}. Here, $F_I^A(A=+,\times,b)$ are the antenna pattern functions of the Ith detector depending on the sky direction and the polarization angle, and representing the detector response to the polarization. $\Psi_{\rm GR}^{(\ell)}$ is the frequency evolution for the ℓth harmonic in GR.

We deal with only the inspiral phase because the merger and ringdown waveforms in a scalar-tensor theory have not yet been constructed for use in a search due to the nonlinearity and complexity of the field equations,

which might lead to large corrections in such a stronger gravity regime [32].

III. ANALYSIS

We analyze the signals of GW170814 [19] and GW170817 [33] in a scalar-tensor polarization framework, which are GW events from a binary black-hole coalescence and a binary neutron-star coalescence observed by three-detector network, respectively. We basically take the same analysis method in [29] and analyze the data under the scalar-tensor hypothesis $\mathcal{H}_{\rm ST}$, in which the GW signal is described as Eq. (5). In addition to A_{S2} and A_{S1}, we consider 13 source parameters: the right ascension and declination of the compact binary system, α and δ, the inclination angle of the binary system ι, the polarization angle ψ, the luminosity distance to the compact binary system d_L, the time and phase at the coalescence, $t_{\rm c}$ and $\phi_{\rm c}$, detector-frame masses, m_1 and m_2, dimensionless spins of the primary and the secondary objects for aligned spin binaries, χ_1 and χ_2, and the tidal deformability parameters of the primary and secondary stars, Λ_1 and Λ_2. However, we do not consider the scalar dipole mode in the analysis of GW170817 for computational cost, because the dipole radiation is already well constrained by the consistency tests for the tensor modes [18,34]. We can translate the constraint on the coefficient shift at -1 post-Newtonian (PN) order $|\delta\hat{\varphi}_{-2}| < 10^{-5}$ for GW170817 [28] into the dipole amplitude $|A_{S1}| \lesssim 0.02$ assuming the relation between them in our model. This is sufficiently smaller than the amplitude determination precision expected from SNR. For GW170814, we need to include the dipole mode because the constraint on the coefficient shift at -1PN order $|A_{S1}| \lesssim 0.02$ [35] corresponds to $|A_{S1}| \lesssim 0.6$, which is comparable to the current sensitivity to the quadrupole scalar amplitude.

Our analysis relies on the Bayesian inference. The posterior probability distribution is calculated from the Bayes' theorem,

$$p(\boldsymbol{\theta}|\{d_I\}_{I=1}^N, \mathcal{H}_{\rm ST}) = \frac{p(\boldsymbol{\theta})p(\{d_I\}_{I=1}^N|\boldsymbol{\theta}, \mathcal{H}_{\rm ST})}{p(\{d_I\}_{I=1}^N|\mathcal{H}_{\rm ST})}. \quad (9)$$

$p(\boldsymbol{\theta})$ represents the prior probability distribution and is basically applied by the standard priors [36] (see the detail in [29]). Since the two amplitudes have different relationships depending on the theory considered, they are treated independently in this analysis. Since we have no specific prior knowledge about the amplitude, we apply uniform priors in the range $[-1, 1]$ for A_{S2} and A_{S1} based on the assumptions made in the construction of the waveform model. $p(\{d_I\}_{I=1}^N|\boldsymbol{\theta}, \mathcal{H}_{\rm ST})$ represents the likelihood function and we apply the standard Gaussian noise likelihood [36]. The lower frequency cutoff for the likelihood calculations is 20 Hz for GW170814 and 23 Hz for GW170817 [36].

We utilize the Bilby software [37,38] and the cpnest sampler [39] for the Bayesian inference. The flat Λ cold dark matter cosmological model is assumed and the cosmological parameters are given in [40]. As an inspiral template, we adopt TaylorF2 [41]

$$\Psi(f) = 2\pi f t_c - \phi_c - \frac{\pi}{4} + \frac{3}{128}(\pi\mathcal{M}f)^{-5/3}\sum_{i=0}^{7}\phi_i(\pi\mathcal{M}f)^{i/3}, \quad (10)$$

where ϕ_c is the phase at the coalescence time t_c and ϕ_i are PN coefficients. For GW170817, we utilize the focused reduced order quadrature technique [42] as in [29]. We use the data of GW170814 whose duration is 4 s and sampling frequency is 4096 Hz and the data of GW170817 with the removal of glitch whose duration is 128 s and sampling frequency is 4096 Hz from the Gravitational Wave Open Science Center [43]. The calibration uncertainties reported in [44] are not considered in the analysis because they are small enough to the statistical errors currently.

As for GW170817, an optical [45] and near-infrared [46] electromagnetic counterpart was observed nearby the galaxy NGC 4993 [47], and the associated gamma ray burst, GRB 170817A, was also observed [48,49]. It is expected that the polarization modes could be more easily separated by strongly restricting the parameter range in advance, from the information on the position and orientation of the binary system independent of the theories of gravity obtained from the observations of the electromagnetic counterparts [29]. In the analysis of GW170817, we additionally impose the location priors on the luminosity distance, the right ascension, and the declination of GW170817 from the position of the host galaxy, NGC4993. The prior of the luminosity distance is set to be the Gaussian distribution with the mean 42.9 Mpc and the standard deviation 3.2 Mpc. We fix the right ascension and the declination to RA $=$ 13h09m48s.085 and DEC $= -23°22'53''.343$ [47]. In addition, the orientation of the compact binary system was also restricted for the viewing angle $\theta_{\rm obs}$ as 0.25 rad $< \theta_{\rm obs}(d_L/41\ {\rm Mpc}) <$ 0.45 rad [50,51]. This can be converted into the inclination angle, $\theta_{\rm obs} = \iota$ or $\theta_{\rm obs} = \pi - \iota$, from the assumption that the jet is perpendicular to the orbital plane of the compact binary system. Consequently, we impose the jet prior on the inclination angle in the range of 2.68 rad $< \iota <$ 2.92 rad [29].

IV. RESULT

For GW170814, Fig. 1 shows the posterior probability distribution for the chirp mass in the detector frame, the luminosity distance, the inclination angle, and the scalar amplitudes under $\mathcal{H}_{\rm ST}$ with 50% and 90% credible intervals. The results under GR are also shown in green for comparison. The distributions for these parameters other

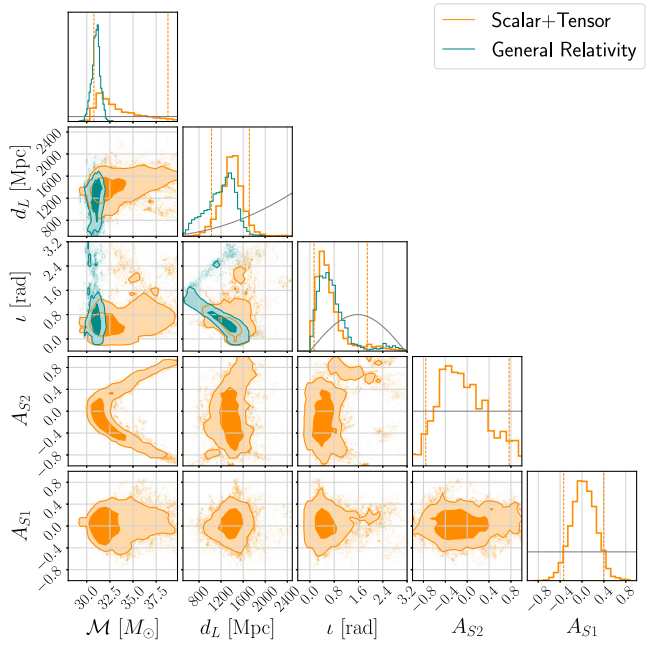

FIG. 1. The posterior probability distributions of the chirp mass in the detector frame, the luminosity distance, the inclination angle, and the scalar amplitudes for GW170814 under the scalar-tensor hypothesis $\mathcal{H}_{\rm ST}$ with 50% and 90% credible intervals in the 2D plots and 90% credible interval in the 1D plots. For comparison, the results under GR are also shown. The priors are shown in gray. The constraint on the scalar amplitude A_{S2} can be converted into the constraint on the ratio of the scalar mode amplitude to the tensor mode amplitude: $R_{\rm ST} \lesssim 0.10$.

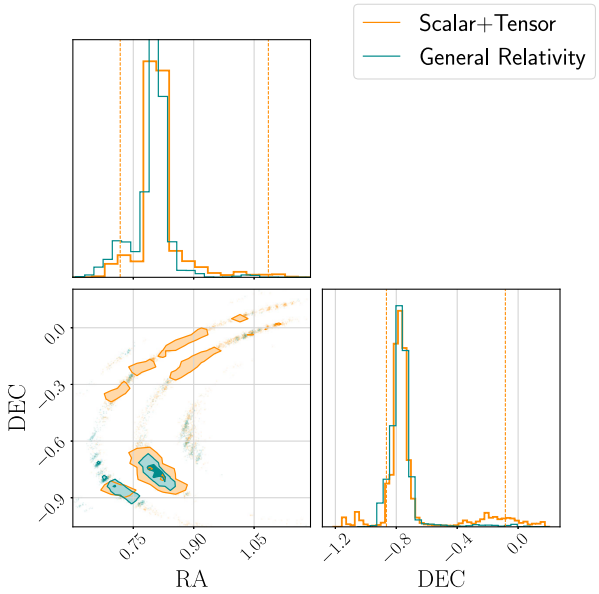

FIG. 2. The posterior probability distributions of GW170814 for the right ascension and the declination are shown in orange under the scalar-tensor hypothesis $\mathcal{H}_{\rm ST}$ and in green under GR. The credible intervals of 50% and 90%, and the credible interval of 90% are shown in the 2D plot and the 1D plots, respectively.

than the scalar amplitude governing the GW amplitude change slightly by adding the scalar mode. The amplitude parameters for the additional scalar modes are constrained by $-0.13^{+0.89}_{-0.63}$ for the quadrupole and $0.03^{+0.37}_{-0.37}$ for the dipole. From the comparison of the amplitude errors estimated from each part of the waveform, we have verified that the contribution from the scalar term dominates compared to the contribution from the phase and amplitude corrections for the tensor modes when the amplitude is small $A_{S2} \lesssim 0.5$. Figure 1 shows that the scalar term starts to be constrained in such a region of small scalar amplitude, shifting the posterior distribution to the negative side slightly. This is because the scalar term compensates for the change in amplitude of the tensor mode with increasing mass, as shown by the 2D correlations. We found the positive 2D correlation between $\mathcal{M}$ and A_{S2} that could come from the amplitude corrections for the tensor modes because the phase part of GW170814 is hardly measured, and then the amplitude correlation still remains. We did not find the strong correlation between the mass ratio and the effective spin. We also did not confirm the strong correlation between the mass ratio and the dipole scalar amplitude, which could be inferred from the expression of the corrections in Eqs. (3) and (4). This suggests that the dipole amplitude is mainly determined directly from the amplitude part, not from the corrections. Figure 2 shows the posterior probability distribution of the right ascension and the declination under $\mathcal{H}_{\rm ST}$ in orange and under GR in green. We found a small but non-negligible change in the posterior, as expected for a small scalar contribution, given that F_b is significantly different from F^+ and $F^\times$.

For GW170817, Fig. 3 shows the posterior probability distributions for the chirp mass in the detector frame, the luminosity distance, the inclination angle, and the scalar amplitude with 50% and 90% credible intervals. The distributions of the chirp mass, the luminosity distance, and the inclination angle also change slightly between under GR and under $\mathcal{H}_{\rm ST}$. The amplitude parameter for an additional scalar mode is constrained in $0.04^{+0.60}_{-0.66}$. In this case, we found the 2D correlation between d_L and A_{S2}. The correlation could be derived from the parameter combination, $(1 - {A_{S2}}^2/3)/d_L$, in the tensor-mode amplitude. This combination of parameters is tightly constrained by the observational data, thereby introducing correlations between d_L and A_{S2}. On the other hand, we did not find the 2D correlation between $\mathcal{M}$ and A_{S2}. The positive correlation between $\mathcal{M}$ and A_{S2} from the amplitude and the negative correlation $\mathcal{M}$ and A_{S2} from the phase would solve the degeneracy between them. We also found the strong correlation between the mass ratio and the effective spin as in [52]. However, there are no strong correlations between A_{S2} and such parameter.

The constraints can be translated into the constraints on the ratio of the scalar amplitude to the tensor amplitude defined for our scalar-tensor waveform model by [53]

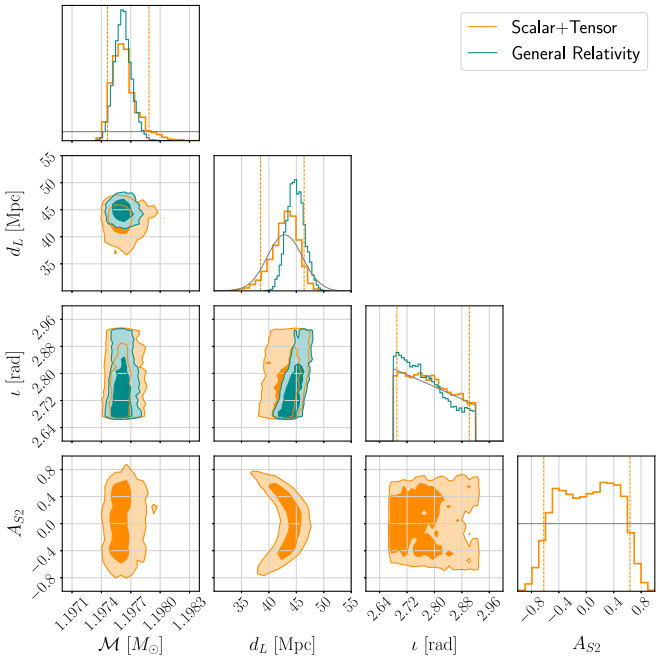

FIG. 3. The posterior probability distributions of the chirp mass in the detector frame, the luminosity distance, the inclination angle, and the scalar amplitude for GW170817 under the scalar-tensor hypothesis $\mathcal{H}_{\rm ST}$ with 50% and 90% credible intervals in the 2D plots and 90% credible interval in the 1D plots. For comparison, the results under GR are also shown. The priors are shown in gray. The constraint on the scalar amplitude A_S can be converted into the constraint on the ratio of the scalar mode amplitude to the tensor mode amplitude: $R_{\rm ST} \lesssim 0.034$.

$$R_{\rm ST} := \left| \frac{A_{S2}\sin^2\iota}{\sqrt{(1+\cos^2\iota)^2 + 4\cos^2\iota}} \right|. \tag{11}$$

This ratio represents how deep the scalar mode is searched in a GW signal. We find the constraints on $R_{\rm ST}$: $R_{\rm ST} \lesssim 0.10$ for GW170814 and $R_{\rm ST} \lesssim 0.034$ for GW170817, which are consistent with GR. This is thought to be because if more scalar waves are emitted, the tensor mode is also significantly deformed and the observed signal cannot be explained. Concomitantly, the distribution of the parameters other than the scalar amplitudes and the location parameters change only slightly. We confirmed that the results do not change significantly with an increased number of live points. The precision of the additional amplitude for GW170814 and GW170817 is comparable, while the amplitude ratio is better determined for GW170817. This comes from the fact that the inclination angle estimated from the gamma ray burst is nearly face-on and the factor $\sin^2\iota$ in the numerator becomes small. The constraint on the scalar coupling in the alternative theories of gravity is given by the additional scalar amplitude A_{S2}, while the amplitude ratio $R_{\rm ST}$ can be regarded as the indicator of the search depth to the polarization modes because the smaller $R_{\rm ST}$ is, the deeper we are able to explore the scalar mode, given the inclination angle.

V. CONCLUSION AND DISCUSSIONS

We searched for mixed scalar-tensor polarization modes of GW170814 and GW170817. We found the constraints on the additional scalar polarization amplitudes, $A_{S2} = -0.13^{+0.89}_{-0.63}$ and $A_{S1} = 0.03^{+0.37}_{-0.37}$ for GW170814 and $A_{S2} = 0.04^{+0.60}_{-0.66}$ for GW170817. These results can be translated into the constraints on the ratio of the scalar amplitude to the tensor amplitude in the GW signals: $R_{\rm ST} \lesssim 0.10$ for GW170814 and $R_{\rm ST} \lesssim 0.034$ for GW170817. Note that since the radiation mechanisms of different physical systems such as binary black holes and binary neutron stars could be different due to the source properties such as a scalar charge or a scalar hair, the two constraints could not be simply compared. This is also the reason why the dipole radiation is ignored in the analysis for GW170817 based on the previous constraints from GW170817 while not for GW170814. The difference between the prior and the posterior on the polarization amplitude parameter can be evaluated by the ratio of the 90% confidence intervals. For GW170814, the ratio of the quadrupole scalar mode is 0.84, and the ratio of the dipole scalar mode is 0.41. For GW170817, the ratio of the quadrupole scalar mode is 0.7. The smaller ratio for the dipole mode could be due to the fact that the dipole mode has a different phase evolution and a larger contribution in the early stage of the inspiral. In addition, the smaller ratio for the quadrupole in GW170817 compared to GW170814 may be due to the additional priors. Since the sensitivity to the polarization amplitude parameter is limited by the detector sensitivity, even in our setup, where the three modes can be separated, in principle, the ratio for the quadrupole is relatively large at this stage, although it is smaller than 1 and consistent with our assumptions.

In the analysis, we only consider the inspiral phase because the merger and ringdown waveform with the scalar polarizations in alternative theories of gravity are not well known. By considering only the inspiral, the estimated luminosity distances are larger than when considering the merger and ringdown phase for GW170814 [36]. In addition, we consider the aligned spin waveform to easily introduce the geometrical patterns for nontensorial radiation. Not considering the precession may result in a loss in the inclination angle and the luminosity distance decomposition. It is possible that the precession may be useful in separating the polarizations depending on the property of the source. It will be a future work to investigate how the precession helps in determining polarizations. Finally, we consider the effect of assuming the stress-energy tensor in GR in the calculation of the energy loss. In order to test the polarization modes with higher sensitivity than the waveform-independent approach using a waveform model that

includes as many theories of gravity as possible, the stress-energy tensor in GR was adopted for the calculation of the energy loss, although the stress-energy tensor can also be modified in the extended gravity theories. This is valid for some theories of gravity, for example, such as the quadratic curvature gravity [54]. As a result, in our model, the corrections also depend on the second order of the polarization amplitude, reflecting that the energy loss is proportional to the second order of the amplitude, as in Eq. (2). On the other hand, however, the stress-energy tensor in the Brans-Dicke theory has a term proportional to the inverse of the coupling, and in the Chern-Simons theory has a term proportional to the scalar field linearly [54,55]. In these cases, the corrections also depend on the coupling included in the scalar amplitude linearly, since the coupling appears linearly in the energy loss. We are currently working on an analysis that takes into account the corrections in the scalar-energy tensor in order to cover more theories.

When the fourth and fifth detector such as KAGRA [56–58] and LIGO India [59] participate in the GW detector network, four and five polarization modes can be probed [21]. Therefore, the expansion of the detector network will make it possible to probe the anomalous GW polarizations directly under a vector-tensor framework or a scalar-vector-tensor framework in the future. On the other hand, the detection limit for the additional amplitude is determined by the SNR. Thus, it is expected that events with larger SNR can be utilized for more precise tests. However, since there is a limit to the accuracy of this test using a single GW event, we are developing a method to statistically combine the polarization analysis results of multiple GW sources.

ACKNOWLEDGMENTS

H. T. acknowledges financial support received from the Advanced Leading Graduate Course for Photon Science (ALPS) program at the University of Tokyo. H. T. is supported by JSPS KAKENHI Grant No. 18J21016. S. M. is supported by JSPS KAKENHI Grant No. 19J13840 and NSF Grant No. PHY-1912649. A. N. is supported by JSPS KAKENHI Grants No. JP19H01894 and No. JP20H04726 and by Research Grants from Inamori Foundation. This research has made use of data, software and/or web tools obtained from the Gravitational Wave Open Science Center [60], a service of LIGO Laboratory, the LIGO Scientific Collaboration, and the Virgo Collaboration. LIGO Laboratory and Advanced LIGO are funded by the United States National Science Foundation (NSF) as well as the Science and Technology Facilities Council (STFC) of the United Kingdom, the Max-Planck-Society (MPS), and the State of Niedersachsen/Germany for support of the construction of Advanced LIGO and construction and operation of the GEO600 detector. Additional support for Advanced LIGO was provided by the Australian Research Council. Virgo is funded, through the European Gravitational Observatory (EGO), by the French Centre National de Recherche Scientifique (CNRS), the Italian Istituto Nazionale di Fisica Nucleare (INFN) and the Dutch Nikhef, with contributions by institutions from Belgium, Germany, Greece, Hungary, Ireland, Japan, Monaco, Poland, Portugal, and Spain.

[1] C. M. Will, *Theory and Experiment in Gravitational Physics* (Cambridge University Press, Cambridge, England, 1993).
[2] I. H. Stairs, Living Rev. Relativity **6**, 5 (2003).
[3] J. Murata and S. Tanaka, Classical Quantum Gravity **32**, 033001 (2015).
[4] C. M. Will, Living Rev. Relativity **9**, 3 (2006).
[5] T. Clifton, P. G. Ferreira, A. Padilla, and C. Skordis, Phys. Rep. **513**, 1 (2012).
[6] C. Brans and R. H. Dicke, Phys. Rev. **124**, 925 (1961).
[7] Y. Fujii and K.-i. Maeda, Classical Quantum Gravity **20**, 4503 (2003).
[8] F. Perrotta, C. Baccigalupi, and S. Matarrese, Phys. Rev. D **61**, 023507 (1999).
[9] D. M. Eardley, D. L. Lee, A. P. Lightman, R. V. Wagoner, and C. M. Will, Phys. Rev. Lett. **30**, 884 (1973).
[10] T. P. Sotiriou and V. Faraoni, Rev. Mod. Phys. **82**, 451 (2010).
[11] J. M. Ezquiaga and M. Zumalacárregui, Phys. Rev. D **102**, 124048 (2020).
[12] Z. C. Chen, C. Yuan, and Q. G. Huang, Sci. China Phys. Mech. Astron. **64**, 120412 (2021).
[13] B. P. Abbott *et al.* (The LIGO Scientific Collaboration), Phys. Rev. X **9**, 031040 (2019).
[14] R. Abbott *et al.*, Phys. Rev. X **11**, 021053 (2021).
[15] J. Aasi *et al.*, Classical Quantum Gravity **32**, 074001 (2015).
[16] F. Acernese *et al.*, Classical Quantum Gravity **32**, 024001 (2015).
[17] B. P. Abbott *et al.*, Phys. Rev. X **6**, 041015 (2016).
[18] R. Abbott *et al.* (LIGO Scientific and Virgo Collaborations), Phys. Rev. D **103**, 122002 (2021).
[19] B. P. Abbott *et al.*, Phys. Rev. Lett. **119**, 141101 (2017).
[20] K. Chatziioannou, N. Yunes, and N. Cornish, Phys. Rev. D **86**, 022004 (2012).
[21] H. Takeda, A. Nishizawa, Y. Michimura, K. Nagano, K. Komori, M. Ando, and K. Hayama, Phys. Rev. D **98**, 022008 (2018).

[22] H. Takeda, A. Nishizawa, K. Nagano, Y. Michimura, K. Komori, M. Ando, and K. Hayama, Phys. Rev. D **100**, 042001 (2019).
[23] Y. Hagihara, N. Era, D. Iikawa, A. Nishizawa, and H. Asada, Phys. Rev. D **100**, 064010 (2019).
[24] P. T. H. Pang, R. K. L. Lo, I. C. F. Wong, T. G. F. Li, and C. Van Den Broeck, Phys. Rev. D **101**, 104055 (2020).
[25] S. Goyal, K. Haris, A. K. Mehta, and P. Ajith, Phys. Rev. D **103**, 024038 (2021).
[26] K. Chatziioannou, M. Isi, C. J. Haster, and T. B. Littenberg, Phys. Rev. D **104**, 044005 (2021).
[27] B. P. Abbott *et al.* (LIGO Scientific and Virgo Collaborations), Phys. Rev. Lett. **119**, 161101 (2017).
[28] B. P. Abbott *et al.* (The LIGO Scientific Collaboration), Phys. Rev. Lett. **123**, 011102 (2019).
[29] H. Takeda, S. Morisaki, and A. Nishizawa, Phys. Rev. D **103**, 064037 (2021).
[30] K. Hayama and A. Nishizawa, Phys. Rev. D **87**, 062003 (2013).
[31] A. Nishizawa, A. Taruya, K. Hayama, S. Kawamura, and M.-a. Sakagami, Phys. Rev. D **79**, 082002 (2009).
[32] T. Damour and G. Esposito-Farèse, Phys. Rev. D **54**, 1474 (1996).
[33] B. P. Abbott *et al.*, Phys. Rev. Lett. **119**, 161101 (2017).
[34] T. G. F. Li, W. Del Pozzo, S. Vitale, C. Van Den Broeck, M. Agathos, J. Veitch, K. Grover, T. Sidery, R. Sturani, and A. Vecchio, Phys. Rev. D **85**, 082003 (2012).
[35] B. P. Abbott *et al.*, Phys. Rev. D **100**, 104036 (2019).
[36] B. P. Abbott *et al.* (LIGO Scientific and Virgo Collaborations), Phys. Rev. X **9**, 031040 (2019).
[37] G. Ashton *et al.*, Astrophys. J. Suppl. Ser. **241**, 27 (2019).
[38] I. M. Romero-Shaw *et al.*, Mon. Not. R. Astron. Soc. **499**, 3295 (2020).
[39] J. Veitch, W. D. Pozzo, and C. M. Pitkin, 10.5281/zenodo.825456 (2017).
[40] P. A. R Ade *et al.* (Planck Collaboration), Astron. Astrophys. **594**, A13 (2016).
[41] A. Buonanno, B. R. Iyer, E. Ochsner, Y. Pan, and B. S. Sathyaprakash, Phys. Rev. D **80**, 084043 (2009).
[42] S. Morisaki and V. Raymond, Phys. Rev. D **102**, 104020 (2020).
[43] R. Abbott *et al.* (LIGO Scientific and Virgo Collaborations), SoftwareX **13**, 100658 (2021).
[44] C. Cahillane *et al.*, Phys. Rev. D **96**, 102001 (2017).
[45] D. A. Coulter *et al.*, Science **358**, 1556 (2017).
[46] N. R. Tanvir *et al.*, Astrophys. J. **848**, L27 (2017).
[47] B. P. Abbott *et al.*, Astrophys. J. **848**, L12 (2017).
[48] C. Meegan *et al.*, Astrophys. J. **702**, 791 (2009).
[49] A. von Kienlin *et al.*, Astron. Astrophys. **411**, L299 (2003).
[50] K. P. Mooley, A. T. Deller, O. Gottlieb, E. Nakar, G. Hallinan, S. Bourke, D. A. Frail, A. Horesh, A. Corsi, and K. Hotokezaka, Nature (London) **561**, 355 (2018).
[51] K. Hotokezaka, E. Nakar, O. Gottlieb, S. Nissanke, K. Masuda, G. Hallinan, K. P. Mooley, and A. T. Deller, Nat. Astron. **3**, 940 (2019).
[52] B. P. Abbott *et al.* (LIGO Scientific and Virgo Collaborations), Phys. Rev. X **9**, 011001 (2019).
[53] H. Yang, A. Nishizawa, and U.-L. Pen, Phys. Rev. D **95**, 084049 (2017).
[54] L. C. Stein and N. Yunes, Phys. Rev. D **83**, 064038 (2011).
[55] A. Saffer, N. Yunes, and K. Yagi, Classical Quantum Gravity **35**, 055011 (2018).
[56] K. Somiya, Classical Quantum Gravity **29**, 124007 (2012).
[57] T. Akutsu *et al.* (KAGRA Collaboration), Prog. Theor. Exp. Phys. **2021**, 05A101 (2021).
[58] Y. Aso, Y. Michimura, K. Somiya, M. Ando, O. Miyakawa, T. Sekiguchi, D. Tatsumi, and H. Yamamoto (KAGRA Collaboration), Phys. Rev. D **88**, 043007 (2013).
[59] B. Iyer *et al.*, LIGO-India Tech. Rep. (2011), https://dcc.ligo.org/LIGO-M1100296/public.
[60] https://www.gw-openscience.org/.